

MODELING OF IMPEDANCE EFFECTS FOR THE APS-MBA UPGRADE*

R.R. Lindberg, ANL, Argonne, IL 60439, USA and A. Blednykh, BNL, Upton, NY 11973, USA

Abstract

Understanding the sources of impedance is critical to accelerator design, and only becomes more important as vacuum chambers become smaller and closer to the electron beam. The multibend achromat upgrade at the Advanced Photon Source (APS) requires small, 22-mm diameter vacuum chambers and even smaller (6 mm) gaps for the insertion devices, so that both rf heating and wakefield-driven transverse instabilities become important concerns. We discuss modeling the primary sources of geometric impedance using the electromagnetic finite difference codes `GdfidL` and `ECHO`, and how these codes are influencing vacuum and accelerator component design.

INTRODUCTION

The vacuum design of the planned multi-bend achromat (MBA) upgrade at the APS must consider many often competing factors. First, the pumping must be able to achieve an ultra-high ($\lesssim 1$ nTorr) vacuum, which is accomplished using local ion pumps in tandem with distributed pumping provided by high surface sorption materials such as non-evaporative getter (NEG) coatings. Second, engineers must find a way to handle the high heat loads associated with synchrotron radiation, both to maintain component integrity and to limit photon-stimulated desorption of gas molecules from the chamber walls. Third, the chambers must be compatible with the magnet design, and permit efficient extraction of bending magnet and undulator radiation for science.

While there are other vacuum design considerations, this list is sufficient to show that the desires of vacuum engineers are typically in conflict with those of an accelerator physicist interested in minimizing beam related wakefields/impedances. These wakefields result from changes in vacuum chamber geometry, and can lead to damaging levels of rf-heating and/or intensity-dependent instabilities. Here, we discuss our efforts to model the geometric sources of impedance associated with the MBA, and how our results are informing vacuum design.

MBA IMPEDANCE MODEL

We analyze the geometric impedance of the MBA using three basic steps. First, we try to identify the primary sources of impedance associated with a particular vacuum design. Second, we use electromagnetic codes to numerically calculate the wakefields associated with each impedance element. Third, we assess the effects of the wakefields on rf heating and beam stability. The next few paragraphs will discuss each of these steps in more detail.

* Work supported by the U.S. Department of Energy, Office of Science, Office of Basic Energy Sciences, under Contract No. DE-AC02-06CH11357.

Table 1: Elements that contribute to the geometric impedance (BPM = beam position monitor).

Sector ($\times 40$)		Ring	
Element	Num.	Element	Num.
BPM	12	Inject. kicker	4
ID BPM	2	Extract. kicker	4
ID transition	1	Feedback	2
Bellow	14	Stripline	1
Flange gap	52	Aperture	2
Crotch abs.	2	Fund. cavity	12
In-line abs.	12	Rf transition	4
Gate valve	4	Harm. cavity	1

We identify potential sources of impedance by drawing heavily on our experience with the present APS impedance model [1], since this model has shown rather good agreement with experimentally measured collective effects at the APS storage ring. We have found that important sources of impedance include both those from large changes in geometry, such as the insertion device (ID) transitions and injection/extraction kickers, and from relatively small perturbations that occur many times in the ring, like the bellows and flange gaps. We list the elements that presently compose the MBA impedance model in Table 1.

We then numerically simulate each impedance element to extract the longitudinal and transverse wakefields. We employ the 2D `ECHO` code [2] to solve for wakefields in axially symmetric elements, which presently include the flange gaps and in-line photon absorbers. Structures without axial symmetry are analyzed using the 3D commercial code `GdfidL` [3]. `ECHO` directly outputs wakefields of a given multipole order (we require the $m = 0$ longitudinal and transverse dipole wakes), while we derive the transverse dipole, quadrupole, and monopole wakefields from `GdfidL` output after a small amount of post-processing.

Finally, we assess the effects of wakefields using a combination of analytic tools and tracking-based simulations. We apply analytic expressions such as the loss factor to obtain important information regarding the energy loss and potential rf-heating issues, and the tracking code `elegant` [4] to predict detailed information regarding the influence of collective effects on beam stability. Note that the numerically calculated wakefields are actually those excited by a Gaussian bunch of duration σ_b , which in turn yields an impedance whose high-frequency components are suppressed by a Gaussian filter of width $1/\sigma_b$. Several test cases have shown that the predicted collective effects are independent of σ_b provided $\sigma_b \leq 1$ mm, and we use the bunch length $\sigma_b = 1$ mm for all wakefield simulations. More details on the tracking results can be found in [5].

Content from this work may be used under the terms of the CC BY 3.0 licence (© 2015). Any distribution of this work must maintain attribution to the author(s), title of the work, publisher, and DOI.

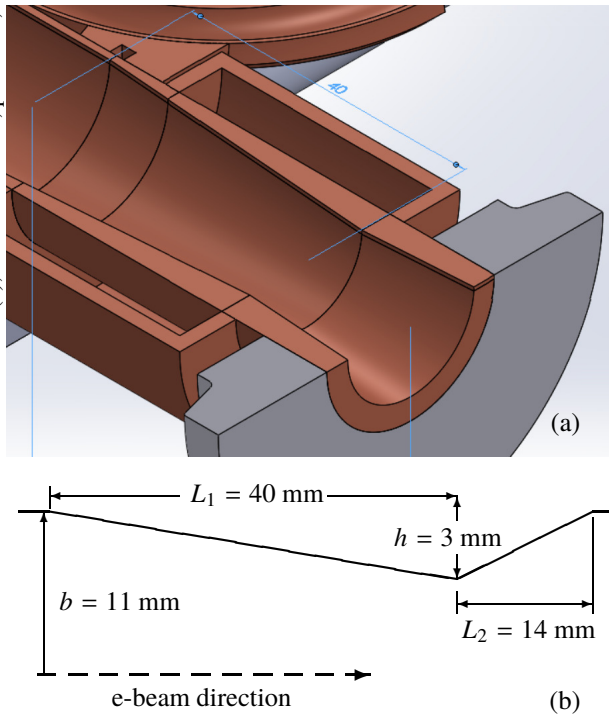


Figure 1: Preliminary design of the in-line photon absorber for the FODO section (a), with dimensions in (b).

PHOTON ABSORBERS

Our preliminary in-line photon absorber design is inspired by the MAX-IV bellows absorber [6]; a picture of the absorber designed for the FODO section is shown in Fig. 1(a). The current plan calls for 5 such absorbers per sector. It serves primarily to protect the BPM and bellows assembly from synchrotron radiation heat loads, and to improve the vacuum by reducing photon-stimulated desorption from the chamber walls. The other 7 absorbers per sector are similar in height and shape, but since their synchrotron radiation heating is much less they do not require water cooling and can be shorter in length. Figure 1(b) shows that the absorber as designed is essentially a tapered collimator from the perspective of impedance, and hence it is instructive to compare the absorber impedance with that of the ID tapered transitions.

In the small angle limit (which is only marginally satisfied for the trailing slope of the absorber), the low-frequency longitudinal impedance of the absorber can be obtained from Yokoya's formula [7] for tapered structures:

$$Z_{\parallel}(k) \approx -ik \frac{Z_0}{4\pi} \frac{h^2(L_1 + L_2)}{L_1 L_2}. \quad (1)$$

For comparison, an approximate expression for the ID transition can be obtained from (1) by making the replacements $h \rightarrow (b - g)$ and $L_1, L_2 \rightarrow L_{\text{trans}}$, where $g = 3$ mm is the ID half-gap, and $L_{\text{trans}} = 185$ mm is the length of the transition.

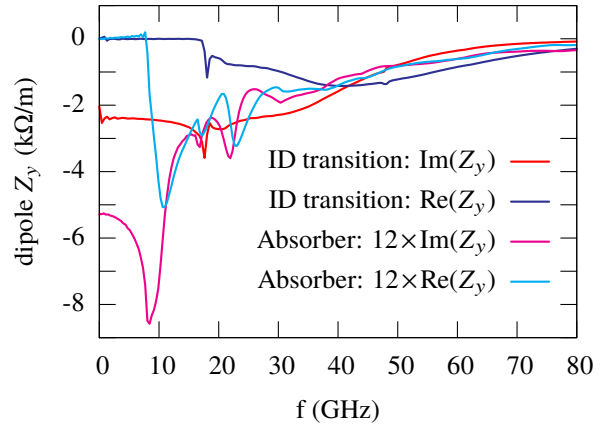


Figure 2: Comparison of the dipole impedance Z_y over one sector for one ID tapered transition and twelve in-line photon absorbers.

Then, we find that

$$\frac{Z_{\parallel}^{\text{abs}}}{Z_{\parallel}^{\text{trans}}} \approx \frac{h^2(L_1 + L_2)}{L_1 L_2} \frac{L_{\text{tran}}}{2(b - g)^2} \sim 1, \quad (2)$$

and the contribution to the longitudinal impedance from one in-line photon absorber is of order that of the ID transition. Since the present design calls for 12 in-line absorbers for every 1 ID transition, the absorbers constitute a major source of longitudinal impedance and driving source of the microwave instability.

Similar considerations show that the low-frequency $Z_{\perp}^{\text{abs}}/Z_{\perp}^{\text{trans}}$ is between 0.1-0.3, depending on how one approximates the 22×22 mm round to 6×20 mm elliptical ID transition. We plot a more complete comparison between the transverse dipole impedances over one sector in Fig 2; since there are 12 in-line absorbers, the impedance Z_y of the absorber is larger than that of the ID transition. Hence, the in-line photon absorbers constitute a major source of both longitudinal and transverse impedance. Unfortunately, the number of these absorbers is still not sufficient to completely shield the vacuum chamber walls from synchrotron radiation, and other simulations indicate that the resulting levels of photon-stimulated desorption lead to an undesirably low gas-scattering lifetime [8].

Because of the sub-optimal vacuum performance and high impedance cost, the vacuum group has begun investigating design alternatives to the seven absorbers per sector that are not in the FODO section (redesign in the FODO section is more challenging due to the water-cooling demands). One attractive option adds a small slot/pocket to the out-board side of the extrusion, within which photon absorbers sit. Because the height of the absorber will now be dictated by the depth of the slot, the slot/pocket design can shadow longer chamber lengths while simultaneously increasing the distance of the absorber from the beam. Hence, it may provide an improved vacuum/e-beam lifetime at a smaller impedance cost: preliminary calculations indicate that the

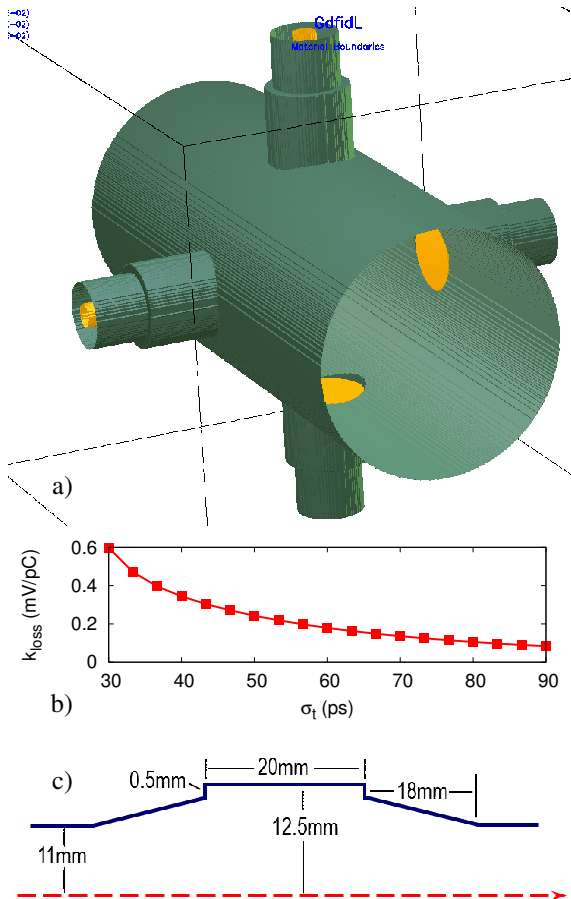


Figure 3: (a) BPM button assembly and (b) loss factor. (c) Simplified 2D bellows geometry

longitudinal impedance contribution of each absorber can be reduced by a factor of ~ 500 , and further mechanical and thermal analysis of this design is underway.

BPM AND BELLOWS ASSEMBLY

Analysis of the large-aperture BPM button started from the simple model shown in Fig. 3(a). The BPM button is 1 mm thick with an 8 mm diameter, while the pin diameter is taken to be 2.4 mm. As a first step, we estimated the energy loss due to wakefields produced by an electron bunch of length $\sigma_z = 15$ mm ($\sigma_t \approx 50$ ps). This length approximately equals the predicted bunch length when the bunch-lengthening higher-harmonic cavity (HHC) is operational if any additional lengthening due to impedance is neglected. We predict that the lowest resonance mode due to the button geometry has a frequency $f_{H11} = 11.6$ GHz (if there is no ceramic material), so that the resonant BPM modes are above the spectrum of the 50-ps bunch. The estimated geometric loss factor from Fig. 3(b) is $k_{\text{loss}} = 0.23$ mV/pC, which results in an estimated power loss of $P_{\text{loss}} = 0.7$ W per BPM assembly in 48 bunch mode at 200 mA. This level of rf-heating appears to be manageable, but it almost doubles if the HHC is off and $\sigma_t \rightarrow 35$ ps.

The present plans for the bellows employs beryllium-copper rf-meshed fingers whose thickness, length, and sep-

aration are 0.5 mm, 18 mm, and 0.2 mm, respectively. For sufficiently long bunches, the bellows geometry can be represented by the axially symmetric 2D model sketched in Figure 3c. We have found that this representation gives a reasonable approximation to the generated wakefields for electron bunches as short 1 mm long, so that the spaces between the rf-fingers contribute very little to the impedance. The next step is to estimate the impedance of the bellows when the rf-fingers are vertically offset by an amount within the required specifications of ± 0.5 mm, and to determine to what extent elevated temperatures might affect the rf finger contact with the inner surface of the vacuum chamber.

However, our previous discussion assumes that the rf fingers make good contact with the bellows and that the BPM buttons are well-centered. If not, local heating can deform the components and potentially cause failure. It is very difficult to accurately model these issues with simulation, so that plans are being made to investigate them experimentally. In addition, the vacuum group is exploring other designs, including options that have external rf liners.

CONCLUSIONS AND FUTURE WORK

Impedance simulations have already provided important feedback for the APS MBA upgrade vacuum design, in particular for the photon absorber and BPM-bellows design. This effort will continue as the MBA design evolves and matures. The present R&D effort also plans to employ experimental measurements, including bench and beam-based measurements, to complement these simulations. In particular, there are plans for rf measurements of the BPM-bellows assembly, gate valves, and flanges, in addition to impedance measurements of a NEG-coated copper chamber to verify its suitability for the FODO section. Finally, the hope is to put these components into the APS storage ring for realistic beam tests at half the average current of the MBA upgrade.

ACKNOWLEDGMENTS

We thank the APS-U Vacuum group (B. Stillwell in particular) for their detailed vacuum design, and M. Borland, Y.-C. Chae, and G. Waldschmidt for useful discussions.

REFERENCES

- [1] Y. Chae et al. *Proc. of PAC 2007*, 4336–4338 (2007).
- [2] I. A. Zagorodnov et al. *Phys Rev ST Accel Beams*, 8:042001 (2005).
- [3] W. Bruns. The GdfidL Electromagnetic Field simulator.
- [4] M. Borland. ANL/APS LS-287, Advanced Photon Source (2000).
- [5] R. R. Lindberg et al. *TUPJE077, IPAC15, these proceedings*.
- [6] MAX IV Detailed Design Report.
- [7] K. Yokoya. SL/90-88 (AP), CERN (1990).
- [8] M. Borland et al. *MOPMA008, IPAC15, these proceedings*.